The control of inorganic nanotube morphology using an applied potential

2011 J. Phys.: Condens. Matter 23 135306

(http://iopscience.iop.org/0953-8984/23/13/135306)

IOP Publishing Journal of Physics: Condensed Matter

J. Phys.: Condens. Matter **23** (2011) 135306 (6pp) doi:10.1088/0953-8984/23/13/135306

The control of inorganic nanotube morphology using an applied potential

Todd R Gingrich[1] **and Mark Wilson**

Department of Chemistry, Physical and Theoretical Chemistry Laboratory, University of Oxford, South Parks Road, Oxford OX1 3QZ, UK

E-mail: mark.wilson@chem.ox.ac.uk

Received 17 January 2011, in final form 23 February 2011
Published 17 March 2011
Online at stacks.iop.org/JPhysCM/23/135306

Abstract

Molecular dynamics computer simulations of the filling of carbon nanotubes (CNTs) by a generic molten salt to form hexagonal-net-based inorganic nanotubes (INTs) are described. A model is introduced to incorporate CNT metallicity which imposes variable Gaussian charges on each atomic site in order to retain an equipotential. The inclusion of CNT metallicity is observed to have no significant effect on the distribution of the INT morphologies formed as compared with the filling of non-metallic CNTs. The application of a voltage bias to the CNT forms a new class of INTs which can be considered as constructed from concentric layers of pseudo-close-packed anions and cations. Removal of the voltage bias leads to the formation of hexagonal-net-based INTs with a distribution of morphologies different to that observed for the filling of the unbiased CNTs. The differences in distributions are interpreted in terms of the CNTs behaving as effective energy landscape filters, for which the applied voltage acts as an additional control variable. The application of a potential acts to control the distribution of INT morphologies by facilitating alternative mechanistic pathways to nanotube formation.

(Some figures in this article are in colour only in the electronic version)

The effective control of the formation of nanostructural materials, here exemplified by pseudo-one-dimensional nanotubes, remains a key technological goal. For nanotubes, fundamental physiochemical properties can only be fully exploited if specific morphologies can be readily isolated. However, the extreme conditions often required to produce such tubular structures [1] appears incommensurate with the holy grail of close morphological control. An alternative synthetic pathway is to use existing nanotubes as *templates*. The advantage of this scenario is that relatively mature research fields, such as the control of carbon nanotube (CNT) morphology, may be exploited to aid the formation of new tubular structures. To this end a wide range of molten salts have been used to fill carbon nanotubes (see [2] for a comprehensive list). Molten salts represent a useful class of filling precursor as their surface tensions are typically low enough so as to avoid crushing the immersed CNT. Filled CNTs have recently been shown as viable systems for radiochemical delivery [3]. Although carbon nanotubes have, to date, been the most common templates, analogous filling experiments have been performed on CsI [4] and PbI_2 [5], both filling WS_2 inorganic nanotubes (INTs). Electron microscopy images indicate that the structures formed within the CNTs are highly ordered. Theoretical (simulation) work has shown that these structures can be considered as belonging to general classes of INT whose morphologies may be understood by reference to the folding of the appropriate (hexagonal- or square-) net sheets [6, 7]. Indeed, the growth in the observation of nanotubular structures for a wide range of materials hints at a ubiquitous nature with such structures occupying metastable regions in the phase diagram.

The computational demands associated with high level (electronic structure) methodologies precludes their effective use in the study of the direct CNT filling, demanding the development of models in which the atomic interactions may be expressed by relatively simple energy functions. Such models allow for the use of the required long length- and timescales and allows for the observation of multiple filling events, potentially giving insight into the statistics and dynamics of nanotube filling [8]. A further attraction

[1] Present address: University of California, Berkeley, College of Chemistry, Berkeley, CA 94720, USA.

of a potential model approach is that model complexity may be built up in a systematic manner, which allows for a proper understanding of the role of specific interatomic interactions on the underlying system properties. For example, detailed pore properties have been shown to control water permeation [9–11]. At the simplest level the CNTs are treated as fixed (rigid, undeformable) atomistic entities which interact with the ions comprising the molten salt via a simple (Lennard-Jones) potential, the parameters for which are obtained by reference to the corresponding isoelectronic noble gas–carbon interactions [12]. At the next level the flexibility of the CNT may be incorporated (most simply by employing an existing bulk carbon potential model [13]). These model extensions influence both INT formation mechanisms and allow for the formation of additional, non-cylindrical, nanocrystalline structures [13, 14]. In all cases, however, the final structures formed are not unique. Instead a distribution of INT morphologies is observed. Information of this sort is often lacking from experimental reports which tend to highlight specific examples of filling morphologies. The implication, therefore, is that such distributions are either as yet unobserved or that the experimental timescales allow the system to find the true free energy minimum. In the MX stoichiometry INTs form with morphologies most generally considered in terms of the folding of infinite sheets of hexagonal- (three-coordinate ions) or square-nets (four-coordinate ions). The INTs may be constructed by folding around a given chiral vector $\mathbf{C}_h = n\mathbf{a}_1 + m\mathbf{a}_2$, where $\mathbf{a}_1$ and $\mathbf{a}_2$ are the unit cell vectors for the sheet, allowing an $(n, m)_X$ notation (X = sq or hex) to describe the INT morphology. The upshot is that the encasing CNTs may be considered as energy landscape filters (ELFs) [14] which act to select INTs from the landscape based largely on the respective CNT/INT radii. In addition, specific mechanistic issues (governing the lowest energy activated pathways by which ions can enter the confining environment) can bias the distribution. For example, INTs of morphology $(n, 0)_{\text{hex}}$ are less often observed than would be expected on a purely radius-based criterion [8].

Key exploitable technological properties concern the system electronic structure. For example, INTs constructed from CdSe (a semiconductor in the ground state bulk wurtzite crystal structure) are expected to have morphology-dependent band gaps [15]. As a result, the ability the control INT morphology is vital if these key properties are to be fully exploited. However, simulation models indicate that single INT morphologies may be near impossible to grow. What is required, therefore, is an understanding of how the distribution of INT morphologies may be best optimized, allowing for a potential *post hoc* separation of the key materials. The requirement to understand the electronic properties motivates a two-pronged simulation strategy. Firstly, the potential model calculations can be used as a direct feed into higher level calculations [15]. Secondly, the potential models themselves may be adapted to incorporate aspects of CNT electronic structure (metallicity). In this paper we focus on the second part of this strategy. The aim of the paper, therefore, is two-fold. Firstly, the effect of including the CNT metallicity will be established. Secondly, the effect of charging the CNT, via the application of a potential bias, will be investigated. One might expect the inclusion of CNT metallicity to have a significant effect both on the filling mechanisms and on the final distribution of INT morphologies formed. The ion–ion Coulombic interactions, which dominate the system energetics, might be expected to be heavily screened by the presence of the metallic wall. CNTs may be semiconducting or metallic, depending upon morphology. A metallic description, therefore, represents the other extreme of behaviour compared with the previous insulating description.

The metallic surface is modelled using variable Gaussian charge on each atomic centre, whose value is tuned to render the electric potential on each site equal [16]. Introducing discrete classical surface charges allows for a good description of even the relatively short-range behaviour of the ion–metal interaction (as tested, for example, by reference to direct electronic structure calculations [17–19]). The use of a Gaussian site charge introduces a single parameter, η, which controls the width of the charge distribution on each site [20, 21]. This parameter ($\eta = 5$ Å^{-1}) is obtained by reference to density-functional calculations on a point-charge/CNT system [19]. The modelling of the metallic CNT in this manner allows a voltage bias to be applied to the metallic sub-system. Significantly, a bias of this type can be applied experimentally (see, for example, [22–24]) and has been shown to promote changes in ionic structure within the CNT [25].

The molten salt is described by a Born–Mayer potential with formal (± 1) ion charges and with the parameters describing the short-range interactions chosen to favour the four-coordinate (wurtzite) crystal structure (and hence favour three-coordinate hexagonal-net-based INTs [6]). The ion–carbon interactions are modelled by a Lennard-Jones potential with parameters obtained by reference to carbon–noble gas interactions [12]. In order to generate significant filling statistics 100 filling events are initiated from independent liquid configurations. Equilibrated liquid configurations are extracted from molecular dynamics simulations performed on the pure MX salt containing 1728 ions at a temperature of 900 K (∼250 K above the estimated melting point [13]). Independent configurations are extracted at time intervals of ∼1 ps, significantly longer than the characteristic system relaxation time associated with ion motions on the length-scale determined by the structure factor principle peak, as monitored by the intermediate scattering function. For each configuration a cylindrical section of salt is removed (retaining charge neutrality) and a fixed CNT (of length ∼15.6 Å) introduced. The final INTs are formed by averaging the ion positions over ∼50 ps (to effectively project out the thermal vibrations about the lattice sites) once the number of ions inside the CNT has equilibrated. The morphologies of the final INTs are identified by determining both the respective chiral angles and radii. Filling simulations are performed using both metallic and non-metallic descriptions of the CNTs. In the present work a single CNT [morphology (11, 11), radius $R \sim 7.5$ Å] is selected as an example of a nanotube in which a relatively low number of INT 'options' are observed [8]. In this case the distributions are dominated by INTs of morphology $(4, 3)_{\text{hex}}$, $(5, 2)_{\text{hex}}$ and $(6, 0)_{\text{hex}}$ respectively.

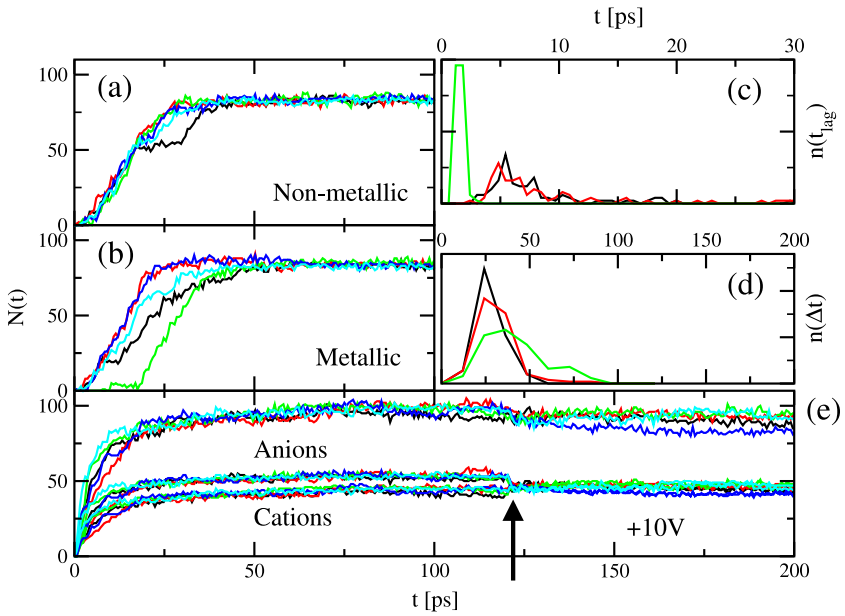

Figure 1. Filling profiles (defined as the total number of ions confined within the CNT as a function of time) generated for the filling of the (11, 11) CNT which is described as (a) non-metallic, (b) metallic with zero bias, and (e) metallic with an applied +10 V bias. In each case five example filling profiles are shown. For the biased metallic CNT (panel (e)) the breakdown into the number of anions and cations is also highlighted. The arrow indicates the time at which the voltage bias was removed. Panels (c) and (d) show the distributions of the filling time (Δt) and lag time ($t_{\rm lag}$), respectively, for the non-metallic (the darkest lines), metallic unbiased (the next lightest [red online] lines) and voltage biased (the lightest [green online] lines) filling simulations. The voltage biased filling events show a significantly shorter lag time and a slightly longer filling time, as described in the text.

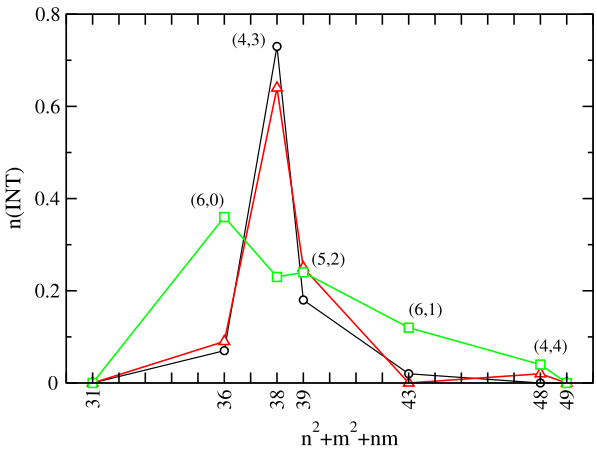

Figure 2. Distribution of INT morphologies obtained in CNTs described as non-metallic (○ symbols), metallic with zero bias (△) and metallic with an applied +10 V bias (square symbol). The abscissa scale is a function of the INT indices and is related to the ideal INT radius, $R = \frac{a_0}{2\pi}(n^2 + m^2 + nm)^{(1/2)}$, with the 'allowed' indices indicated. The individual INT morphologies are also highlighted.

Figures 1(a) and (b) show example filling profiles (the number of ions inside the CNT as a function of time) for the non-metallic and metallic (11, 11) CNTs. In both cases individual filling events are characterized by a lag time ($t_{\rm lag}$—the time from the start of the simulation to the beginning of the salt ingress) and a filling time (Δt—the time from the beginning of the filling to the final plateau, indicative of a stable final structure). The inclusion of CNT metallicity appears to have no significant effect upon the distribution of these quantities. Figures 1(c) and (d) show the distributions of $t_{\rm lag}$ and Δt respectively. For the non-metallic CNT $\overline{t_{\rm lag}}$ and $\overline{\Delta t}$ (standard deviations in parentheses) are 15.9 ps (26.1 ps) and 33.4 ps (7.8 ps) respectively, whilst the corresponding values for the metallic CNT are 17.0 ps (26.7 ps) and 36.5 ps (11.2 ps). Figure 2 shows the distribution of INTs obtained from the metallic and non-metallic CNTs displayed as a function of the $(n, m)_{\rm hex}$ indices related to the ideal INT radius [$R^{\rm INT} = \frac{a_0}{2\pi}(n^2 + m^2 + nm)^{(1/2)}$, where a_0 is the lattice parameter of the sheet precursor]. Again, the distributions appear near-indistinguishable with the $(4, 3)_{\rm hex}$ INT strongly favoured over either the $(5, 2)_{\rm hex}$ or the $(6, 0)_{\rm hex}$ (figure 4(a)). The implication of the filling profiles (figure 1) and the distribution of the final INT structures (figure 2) is that the inclusion of CNT metallicity has no significant effect upon either the filling dynamics or the static structures formed on filling the CNTs.

Figure 3 shows the distribution of the site charges as a function of the distance along the major axis of the CNT. The distribution of charges has zero mean as would be expected for an unbiased CNT in a charge-neutral molten salt. The standard deviation of the induced charge is of the order of $0.005|e|$, that is, charges imposed upon the metal sites in the unbiased CNT appear relatively small. One might expect that the electrostatically driven short-range ordering present in the bipartite INT would induce a charge density wave in the Gaussian charge distribution, complementing that present in the INT itself. This is not the case as the C–C bond length renders the confining CNT incommensurate with the forming INT (at least for the material studied here) and so formation of the charge density wave is discouraged.

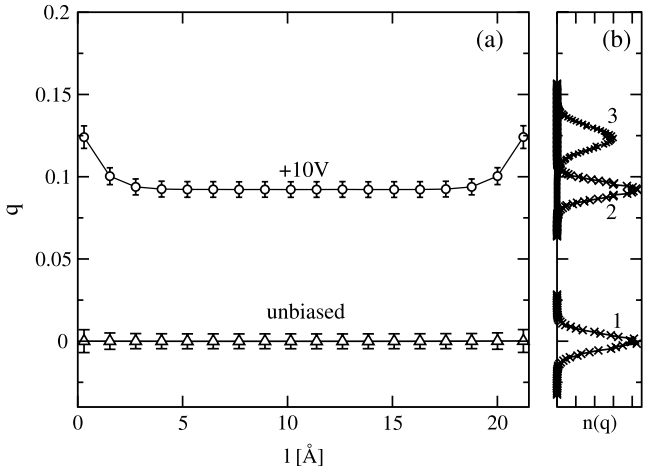

Figure 3. (a) Site charges as a function of distance along the major CNT axis, l, shown for the unbiased and biased CNTs as indicated. The charge standard deviations in each CNT section are also shown. Panel (b) shows the charge distributions at the centre of the unbiased CNT ('1') and at the centre and edge of the biased CNT ('2' and '3' respectively). The greater charge at the CNT edges for the biased CNT, and the greater variance of charge at the edges in both the biased and unbiased tubes, results from the reduced atom coordination environments present at the CNT edges as discussed in the text.

Figure 1(e) shows the filling profiles obtained on filling the (11, 11) CNT with an applied +10 V bias. Two differences (static and dynamic) with respect to the unbiased filling events are noticeable. Firstly, the filling appears initially much more rapid (as seen in the distributions of t_{lag} in figure 1(c)) with $\overline{t_{\mathrm{lag}}} = 1.6$ ps (0.4 ps). However, the distribution of Δt is shifted to slightly longer time, with $\overline{\Delta t}$ as 46.5 ps (17.1 ps), indicating that the final structures form on similar timescales to those in the unbiased nanotubes. Secondly, the number of anions and cations in the final plateau are now different, with figure 3 showing the distribution of charge now present on the CNT. The application of a voltage bias acts to drive the formation of positive charge on the metallic sites. Note that the charge built up at the CNT edges appears larger than that generated in the CNT centre as the result of the lower carbon–carbon coordination environments present at the CNT edges. The same effect is observed in the unbiased CNT as a more subtle increase in the variance of the edge charges (as seen in the error bars in figure 3). The imposition of positive charge on the CNT, as a result of the applied voltage bias, provides a driving force for a layer of anions to effectively wet the inner CNT wall with a further layer of cations wetting this inner anion layer. The anion and cation sublattices can, therefore, be considered as forming separate (single ion) inorganic nanotubes. As a

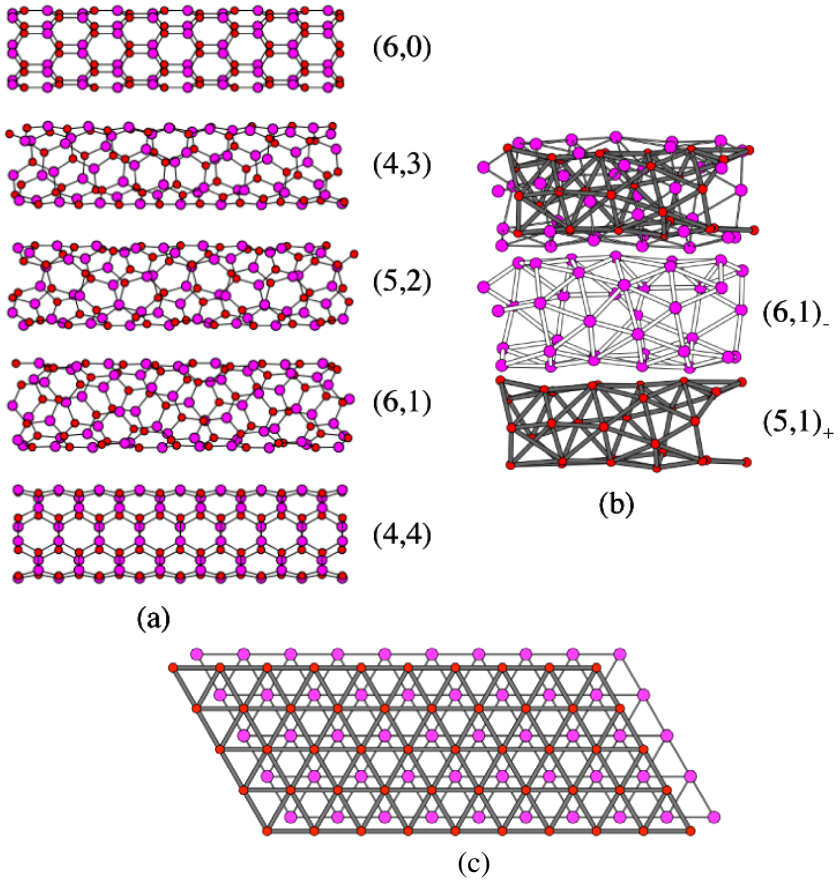

Figure 4. Molecular graphics 'snapshots' of the INT structures formed in the (a) unbiased CNT and (b) voltage biased CNT. The labels indicate the INT morphologies as explained in the text. For the biased tube the complete INT (upper panel) comprised concentric single-walled INTs as highlighted by the lower panels. Panel (c) shows how the two sublattices ideally overlap in order to maximize the unlike interactions.

result, the radius of the inner cation INT is smaller than that of the outer anion analogue (of the order of 3.1 Å and 3.9 Å respectively) and hence contains fewer ions.

The differences in the distributions of t_{lag} and Δt with and without the applied voltage bias are indicative of a fundamental change in the primary filling mechanism. For the unbiased tube the ions enter the CNT in a highly correlated manner as 'loops' of charge-neutral anion–cation–anion$\cdots$ chains [13]. The dominant factor in the relatively low activation energies associated with this motion is the relative ease of moving charge-neutral (chain) structures around as opposed to moving single ions themselves. On applying a voltage bias the ions are able to move into the CNT in a less correlated manner, often as single entitles. The positive charge generated on the CNT surface act to promote the motion of single negative ions into the CNT. This uncorrelated single ion motion is much more rapid than the highly correlated motion of the ion chains, resulting in shorter filling lag times. However, the more rapid initial salt ingress causes a depletion of salt at the nanotube openings which then results in a slightly longer filling time (Δt), as this timescale is diffusion controlled [26].

In addition to displaying markedly distinct dynamics, the simulations with an applied potential resulted in a unique set of concentric INT structures. Both the anion and cation sublattices form INTs whose structures can be rationalized in analogous fashion to the INTs formed in the unbiased CNTs. The INT structures arising from growth in an unbiased CNT have previously been described with respect to the folding of a bipartite hexagonal lattice as shown in figure 4(c). The result is a roughly cylindrical tube consisting of anions and cations. In the case of the biased CNT, however, the charge on the CNT surface breaks the symmetry and serves to push the two sublattices apart as the one set of ions is attracted to the CNT surface and the others are repelled. For a small biasing potential this effect is a perturbation which causes the ordinary INTs to buckle slightly. For a sufficiently large bias, however, the anion and cation sublattices must fold with significantly different radii. As such, the inner tube cannot contain as many ions as its counterpart, hence the anion and cation tubes can no longer perfectly associate. This incommensurability of the lattices leads to defects and distortions, yet the anion and cation tubes can still be effectively categorized by the chiral vector. Figure 4(b) illustrates the concentric tubes for the particular example in which the anion INT has a (6, 1) morphology (referred to as $(6,1)_-$) whilst the cations form a $(5,1)_+$ INT. The final structures represent the result of a balance between maximizing the unlike interactions (i.e. retaining the local complementarity of the sublattices) and minimizing the lattice mismatch. In the $(6,1)_-/(5,1)_+$ pair, for example, the inner cation INT is compressed with respect to the outer anion layer (with mean X–X and M–M separations of 3.81 Å and 3.67 Å respectively). It should be noted that the INTs of figure 4(a) differ from those of figure 4(b) in that the nearest-neighbour interactions of the former are attractive. In contrast, the anion and cation tubes are formed exclusively by repulsive interactions, though there are of course attractive interactions between the inner and outer tubes. Regardless of the attractive or repulsive nature of the interactions, the ions pack into a hexagonal lattice, which is constrained to adopt one of a small number of stable topologies upon folding into a tube. We note that the structures formed by packing hard spheres into rigid cylinders [27] can be rationalized in the same manner.

In order to establish how the single ion INT structures relax into the hexagonal-net-based structures, additional simulations are performed in which the potential bias is removed once the CNTs are fully filled. The effect of this procedure on the filling profiles is indicated in figure 1(e) with the bias removed at $\sim$120 ps from the beginning of the respective simulations. Since the biased metal surface charge is no longer supported, the internal stoichiometry reverts to a simple charge-neutral 1:1, and analysis of the final structures indicate the formation of the hexagonal-net-based INTs. Figure 2 shows that the distribution of the INT morphologies formed are very different to those formed in the unbiased simulations. For the potential biased CNT the final distribution appears broader but the structures appear to be selected from the same subset of available morphologies as for the unbiased tubes.

The applied voltage bias behaves as an additional control variable to the system temperature, with the power to change the final distribution of INT morphologies, yet here it is not acting as a thermodynamic control variable. The final structures form with the potential bias removed, so the thermodynamic parameters during the final relaxation are the same as those used for unbiased growth. Hence the applied voltage has altered the kinetics resulting in a different distribution of structures. The question remains as to whether these distributions are truly experimentally accessible or are simply metastable on typical simulation timescales. It is possible that, over experimental timescales, the less thermodynamically stable INTs may transform into a single stable structure. It is likely, however, that elevated temperatures would be required to promote these INT $\longrightarrow$ INT transformations, reflecting both the relatively high activation barriers associated with ion transport and the relatively low thermodynamic driving forces. As a result, it is likely that the observed distributions are experimentally accessible. While previous reports have demonstrated that much of the complexity of INT formation can be understood through energy minimization and thermodynamic arguments [6, 8, 14], these results suggest that kinetic factors can also play a key role. In particular, it is likely that by driving a system far from equilibrium the dynamical pathway can be dramatically altered to result in a distinct distribution of long-lived metastable states.

In summary, the inclusion of a metallic description of a selected CNT appears to have no significant effect either on the filling dynamics or on the observed distribution of the final (hexagonal-net-based) INT morphologies. The application of a potential bias to the CNT favours the formation of a distribution of a new class of INT whose structures can be considered as formed from concentric cylinders of folded pseudo-close-packed ions. The removal of the potential bias results in the formation of hexagonal-net-based INTs with a distribution of morphologies which differs significantly from that formed in the unbiased cases. As a result, a voltage

bias appears a useful way of effectively controlling the INT morphology distribution.

References

[1] Tenne R, Homyonfer M and Feldman Y 1998 *Chem. Mater.* **10** 3225
[2] Sloan J, Kirkland A I, Hutchison J L and Green M L H 2002 *Chem. Commun.* 1319
[3] Hong S Y *et al* 2010 *Nat. Mater.* **9** 485
[4] Hong S Y, Popovitz-Biro R, Tobias G, Ballesteros B, Davis B G, Green M L H and Tenne R 2010 *Nano Res.* **3** 170
[5] Kreizman R, Hong S Y, Sloan J, Popovitz-Biro R, Albu-Yaron A, Tobias G, Ballesteros B, Davis B G, Green M L H and Tenne R 2009 *Angew. Chem. Int. Edn* **48** 1230
[6] Wilson M 2006 *J. Chem. Phys.* **124** 124706
[7] Wilson M 2004 *Nano Lett.* **4** 299
[8] Wilson M 2009 *J. Chem. Phys.* **131** 214507
[9] Allen R J, Melchionna S and Hansen J-P 2002 *Phys. Rev. Lett.* **89** 175502
[10] Dzubiella J, Allen R J and Hansen J-P 2004 *J. Chem. Phys.* **120** 5001
[11] Allen R J, Melchionna S and Hansen J-P 2003 *J. Phys.: Condens. Matter* **15** S297
[12] Steele W A 1978 *J. Phys. Chem.* **82** 817
[13] Bishop C L and Wilson M 2009 *J. Mater. Chem.* **19** 2929
[14] Bishop C L and Wilson M 2009 *J. Phys.: Condens. Matter* **21** 115301
[15] Mercuri F, Leoni S, Green J C and Wilson M 2010 *Phys. Rev.* B **82** 155429
[16] Gingrich T R and Wilson M 2010 *Chem. Phys. Lett.* **500** 178
[17] Finnis M 1992 *Acta Metall. Mater.* **40** S25
[18] Finnis M, Kaschner R, Kruse C, Furthmüller J and Scheffler M 1995 *J. Phys.: Condens. Matter* **7** 2001
[19] Meunier V, Kalinin S V, Shin J, Baddorf A P and Harrison R J 2004 *Phys. Rev. Lett.* **93** 246801
[20] Siepmann J I and Sprik M 1995 *J. Chem. Phys.* **102** 511
[21] Reed S K, Lanning O J and Madden P A 2007 *J. Chem. Phys.* **126** 084704
[22] Holloway A F, Toghill K, Wildgoose G C, Compton R G, Ward M A H, Tobias G, Llewellyn S A, Ballestoros B, Green M L H and Crossley A 2008 *J. Phys. Chem.* C **112** 10389
[23] Banks C E and Compton R G 2006 *Analyst* **131** 15
[24] Kavan L, Dunsch L and Kataura H 2004 *Carbon* **42** 1011
[25] Vatamanu J, Borodin O and Smith G 2010 *Phys. Chem. Chem. Phys.* **12** 170
[26] Wilson M 2002 *J. Chem. Phys.* **116** 3027
[27] Pickett G T, Gross M and Okuyama H 2000 *Phys. Rev. Lett.* **85** 3652